Spatiotemporal Pattern Formation in a Model of Electrically Coupled Smooth Muscle Cells

Hammed Olawale Fatoyinbo

ANZIAM 2020
Hunter Valley, NSW Australia

MASSEY UNIVERSITY
TE KUNENGA KI PŪREHUROA
UNIVERSITY OF NEW ZEALAND

Overview

Introduction
- Electro-mechanical coupling (EMC)
- Research goals

Model Equations

Single-cell dynamics
- Effect of ion currents on pacemaker activity
- Bifurcation analysis

Spatiotemporal patterns
- Effect of model parameters on spatiotemporal patterns

Summary and future work

Electro-mechanical coupling (EMC)

- Electro-mechanical coupling (EMC) is the contraction of muscle cell as a result of the excitability of the cell membrane in response to an external stimulation.
- In some muscle cells, for example smooth muscle cell (SMC), EMC activity is spontaneous due to ion fluxes in the cell membrane through the voltage-gated ion channels.
- This type of behaviour of the muscle cell is known as *pacemaker dynamics*.

Research goals

Motivation

- *In vivo* studies showed that pacemaker EMC activity observed in a arterial muscle cells depend on transmural pressure.
- Upon elevation of transmural pressure, spontaneous electrical firing is observed and the blood vessel constricts.

Aim

- To investigate mathematically how parameters involved in the equations governing transmural pressure influence the ionic mechanisms and EMC activity of smooth muscle cells in feline cerebral arteries.
- To study the collective behaviour of the SMCs by using a reaction-diffusion system and incorporating gap junction coupling between cells.

Schematic diagram of coupled SMCs

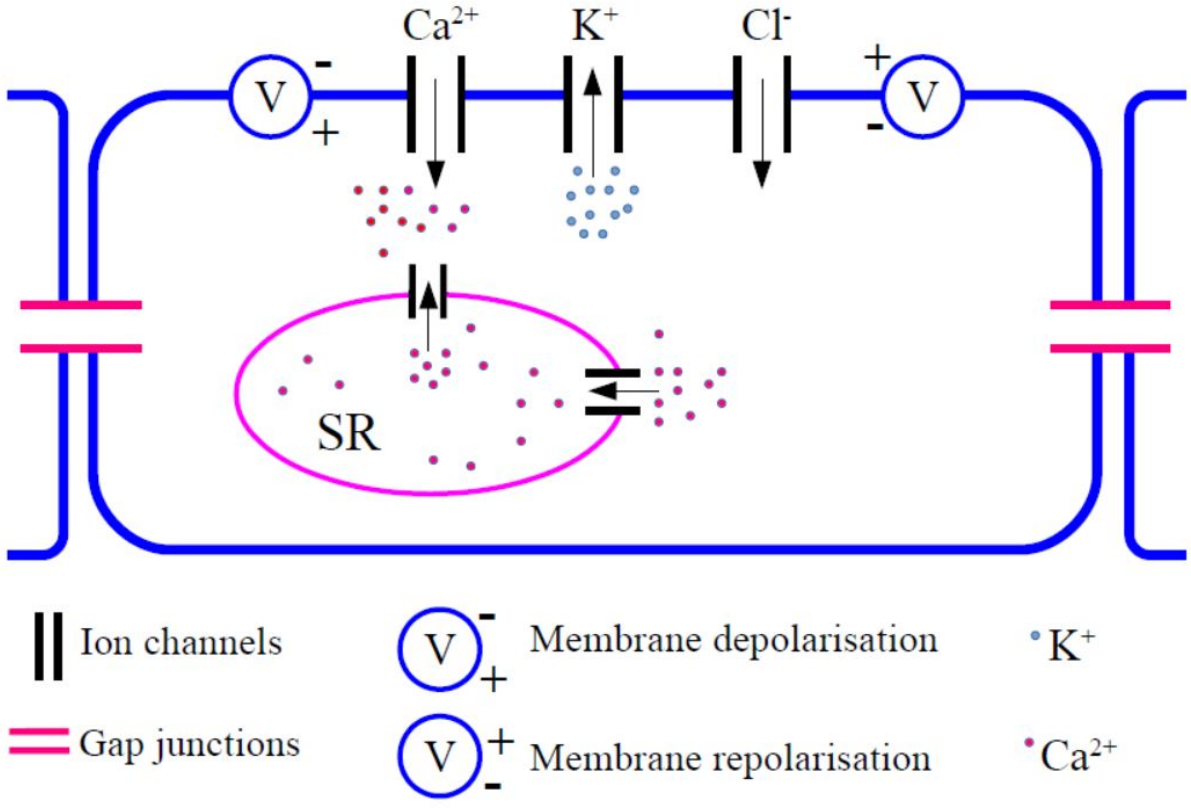

Figure 1: Schematic representation of coupled smooth muscle cells

Model formulation

$$C\frac{dv}{dt} = -g_L(v - v_L) - g_K n(v - v_K) - g_{Ca} m_\infty(v)(v - v_{Ca}), \quad (1)$$

$$\frac{dn}{dt} = \lambda_n(v)\big(n_\infty(v, Ca_i) - n\big), \quad (2)$$

$$\frac{dCa_i}{dt} = \big(- \alpha g_{Ca} m_\infty(v)(v - v_{Ca}) - k_{Ca} Ca_i\big)\rho(Ca_i), \quad (3)$$

where,

$$m_\infty(v) = 0.5\left(1 + \tanh\left(\frac{v - v_1}{v_2}\right)\right),$$

$$n_\infty(v, Ca_i) = 0.5\left(1 + \tanh\left(\frac{v - v_3(Ca_i)}{v_4}\right)\right),$$

$$v_3(Ca_i) = -\frac{v_5}{2}\tanh\left(\frac{Ca_i - Ca_3}{Ca_4}\right) + v_6,$$

$$\lambda_n(v) = \phi_n \cosh\left(\frac{v - v_3(Ca_i)}{2v_4}\right), \quad \rho(Ca_i) = \frac{(K_d + Ca_i)^2}{(K_d + Ca_i)^2 + K_d B_T}.$$

(Gonzaléz-Fernandez and Ermentrout, 1994)

Model reduction

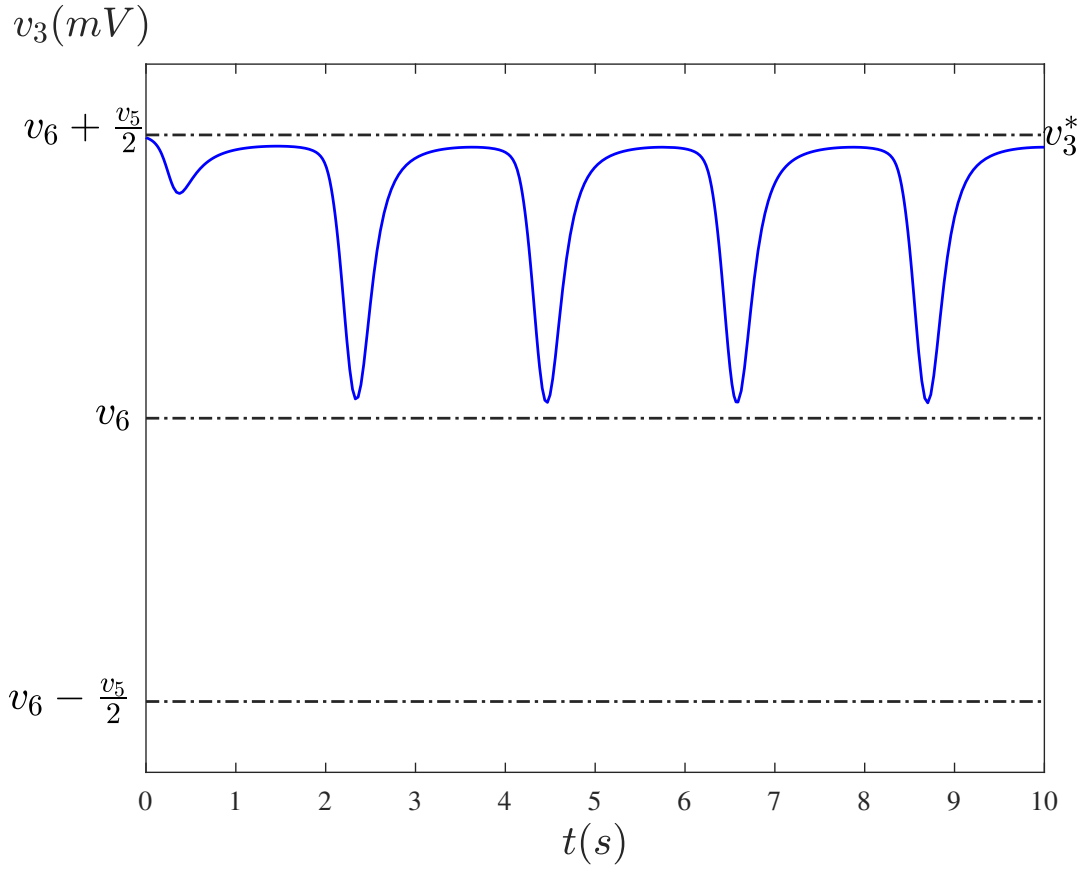

Figure 2: A plot of $v_3(mV)$ against time

Nondimensionalised model

$$\frac{dV}{dT} = -\bar{g}_L(V - \bar{v}_L) - \bar{g}_K N(V - \bar{v}_K) - \bar{g}_{\mathrm{Ca}} M_\infty(V)(V - 1), \tag{4}$$

$$\frac{dN}{dT} = \lambda(V)(N_\infty(V) - N), \tag{5}$$

where

$$M_\infty(V) = 0.5\left(1 + \tanh\left(\frac{V - \bar{v}_1}{\bar{v}_2}\right)\right),$$

$$N_\infty(V) = 0.5\left(1 + \tanh\left(\frac{V - \bar{v}_3}{\bar{v}_4}\right)\right),$$

$$\lambda(V) = \psi \cosh\left(\frac{V - \bar{v}_3}{2\bar{v}_4}\right),$$

and

$$\bar{g}_i = \frac{g_i}{g_K}, \quad \bar{v}_i = \frac{v_i}{v_{\mathrm{Ca}}}, \quad \psi = \frac{C\phi_n}{g_K}, \qquad i = L, K, \mathrm{Ca}, 1, 2, 3, 4.$$

Effect of ion currents on pacemaker activity

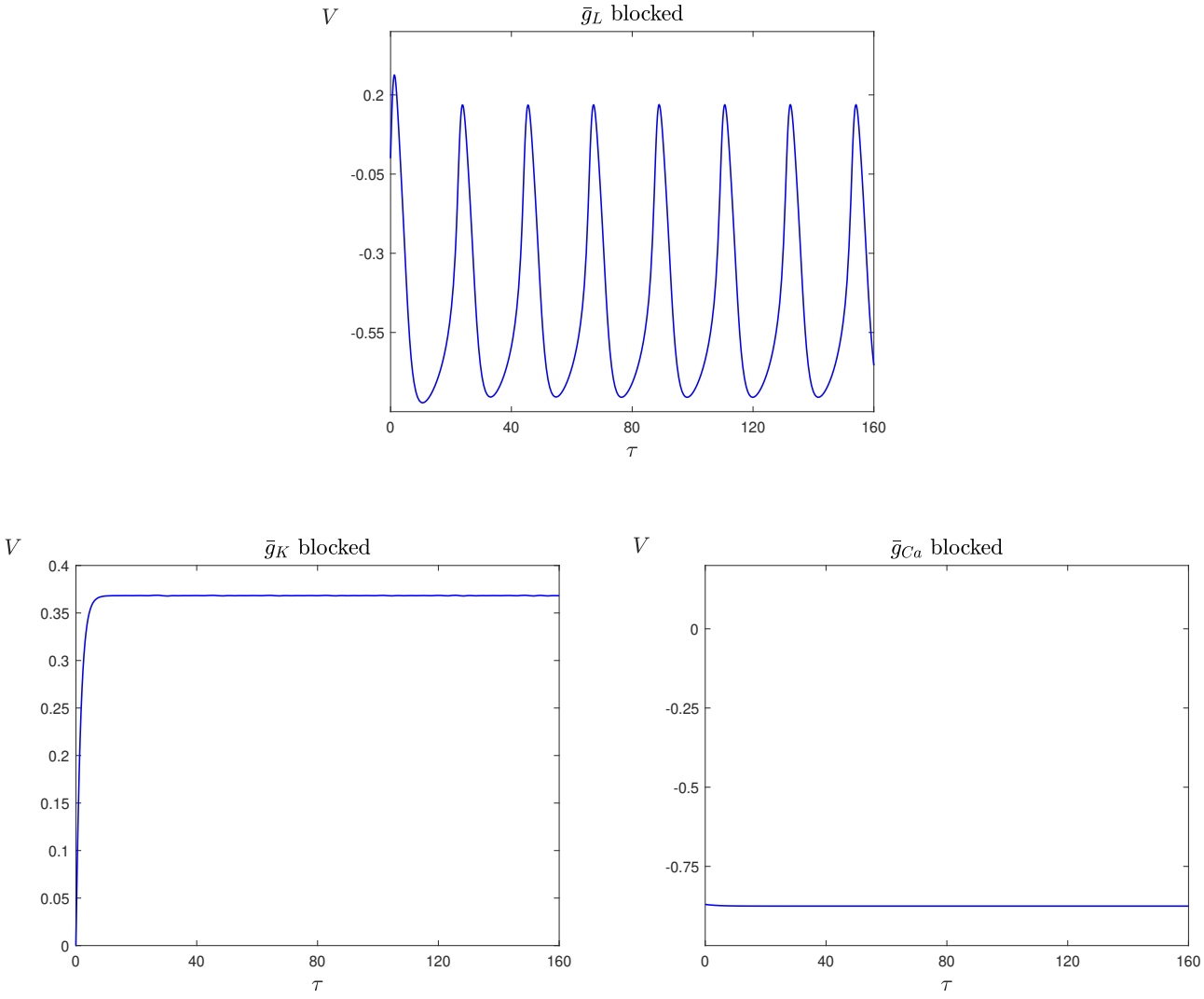

Figure 3: Plots of the nondimensionalised model when the conductance for the (a) leak (b) potassium and (c) calcium- channels are blocked, respectively.

Nullclines

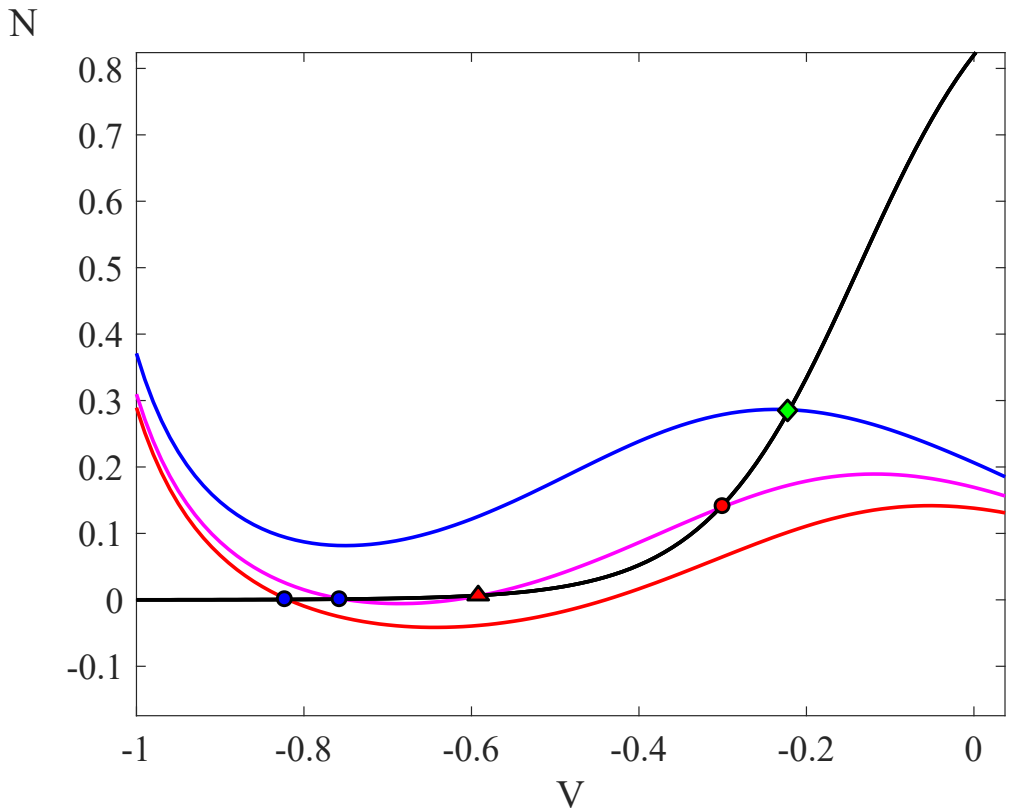

Figure 4: The two nullclines of model for three different values of $\bar{v}_1$. Varying $\bar{v}_1$ shifts V-nullcline up or down

Bifurcation analysis

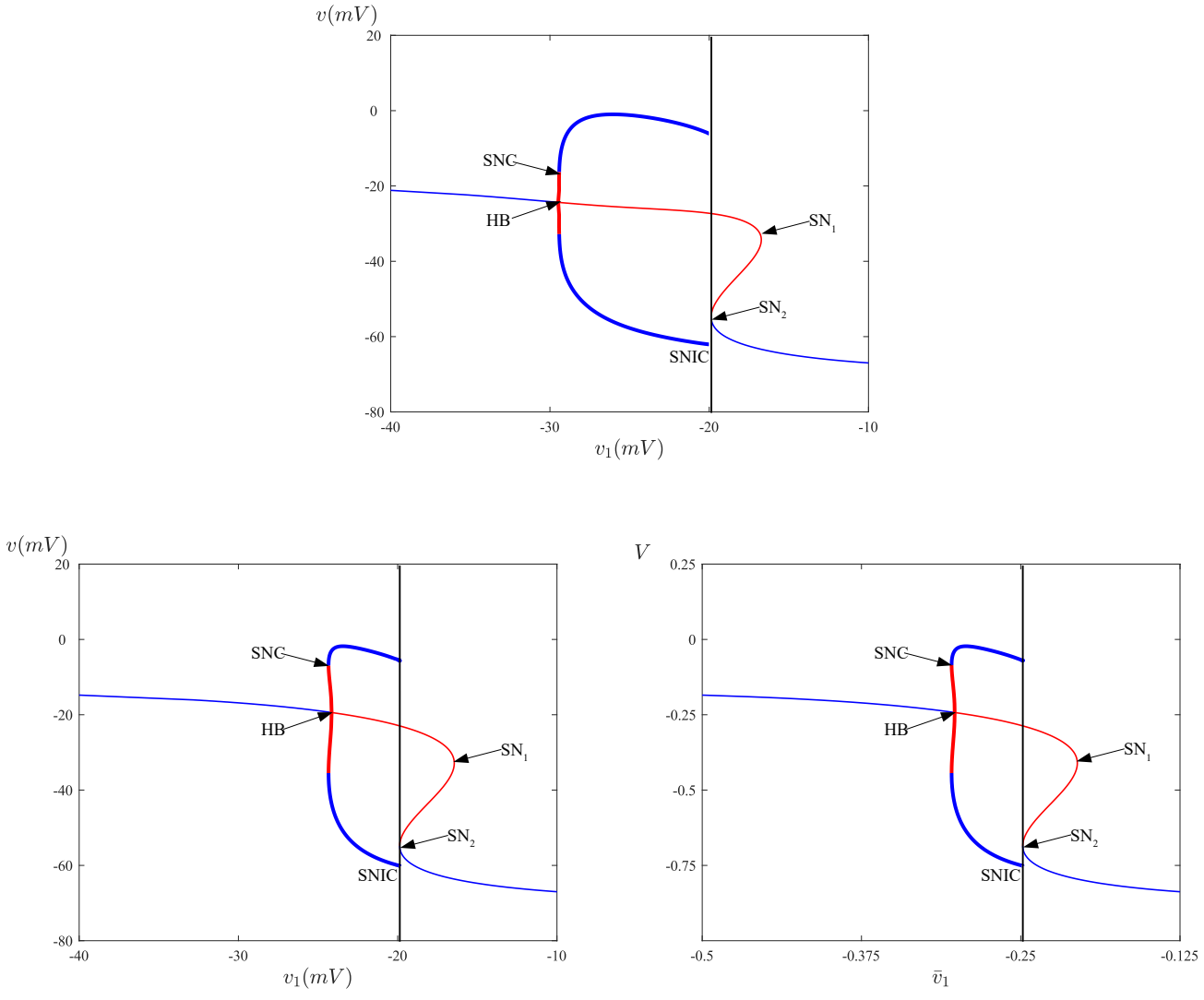

Figure 5: Bifurcation diagram of the membrane potential for the full, reduced and nondimensionalised models with v_1 and $\bar{v}_1$ as the bifurcation parameters.

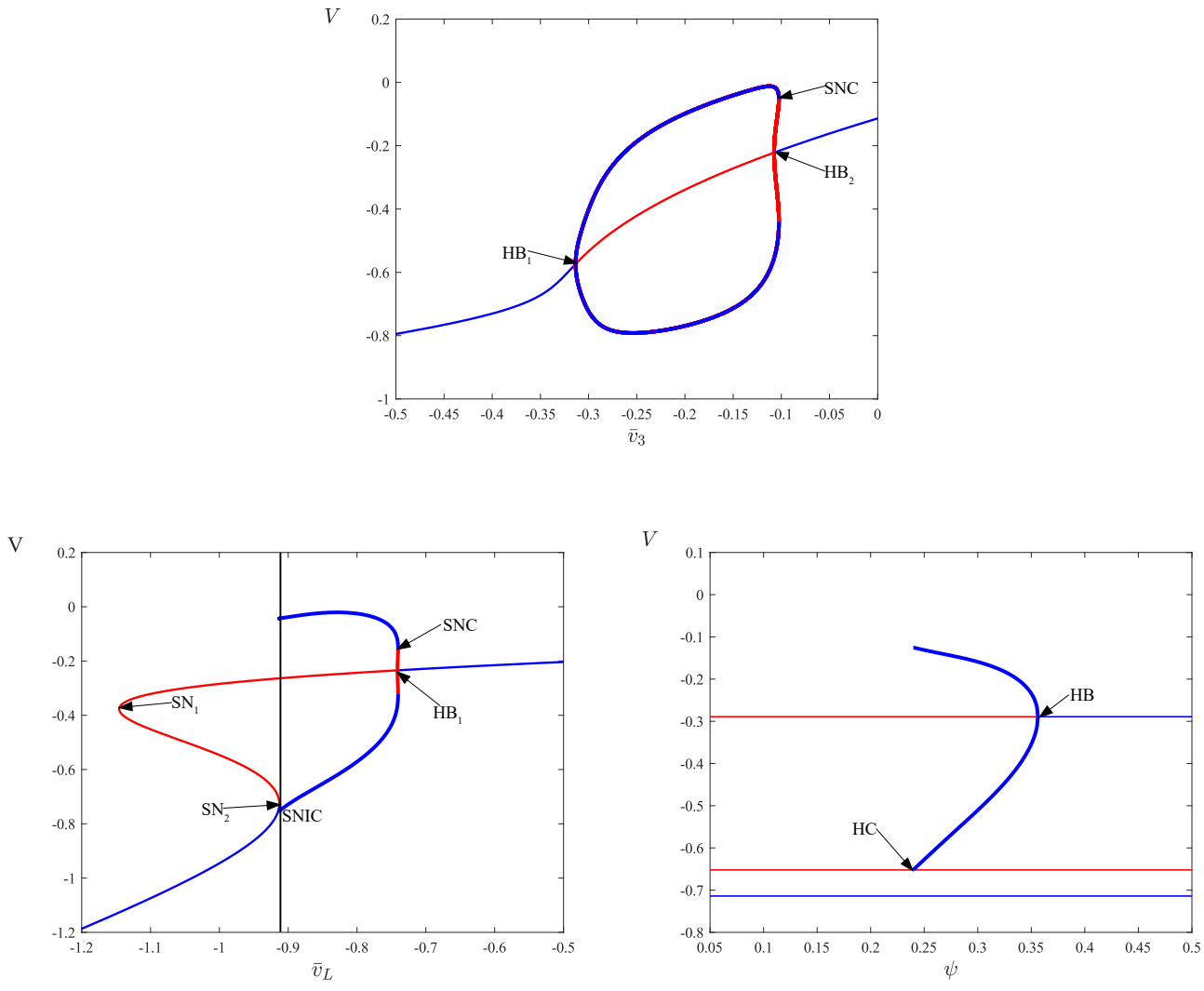

Figure 6: Bifurcation diagram of the membrane potential with $\bar{v}_L$, $\bar{v}_3$, and ψ as bifurcation parameters respectively.

$(\bar{v}_1, \bar{v}_3)$ parameter plane

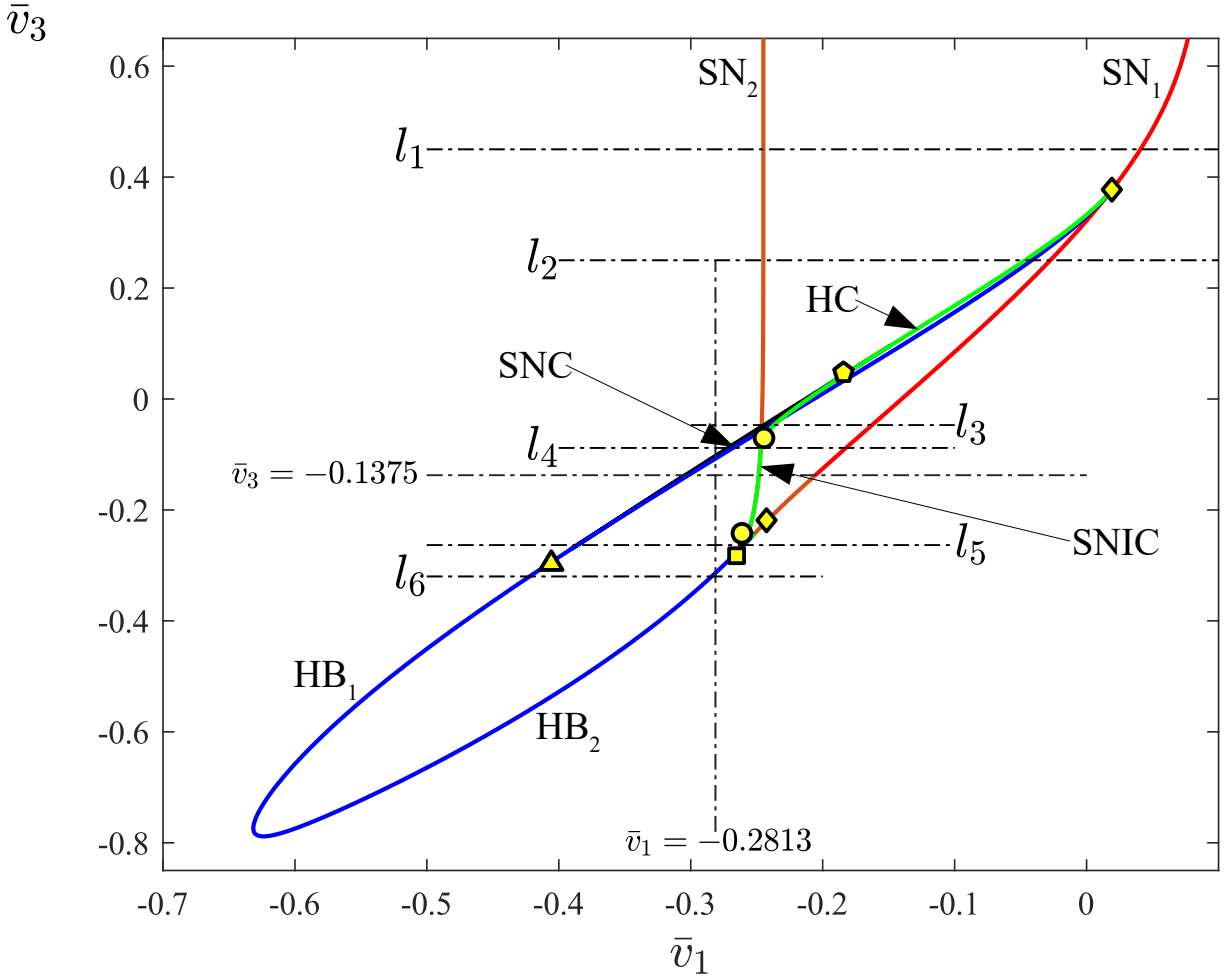

Figure 7: The filled square, diamond, triangle, pentagon and circle refers to the cuspid bifurcation point, Bodganov-Takens bifurcation and generalised Hopf bifurcation, resonant homoclinic and non-central saddle homoclinic bifurcation respectively.

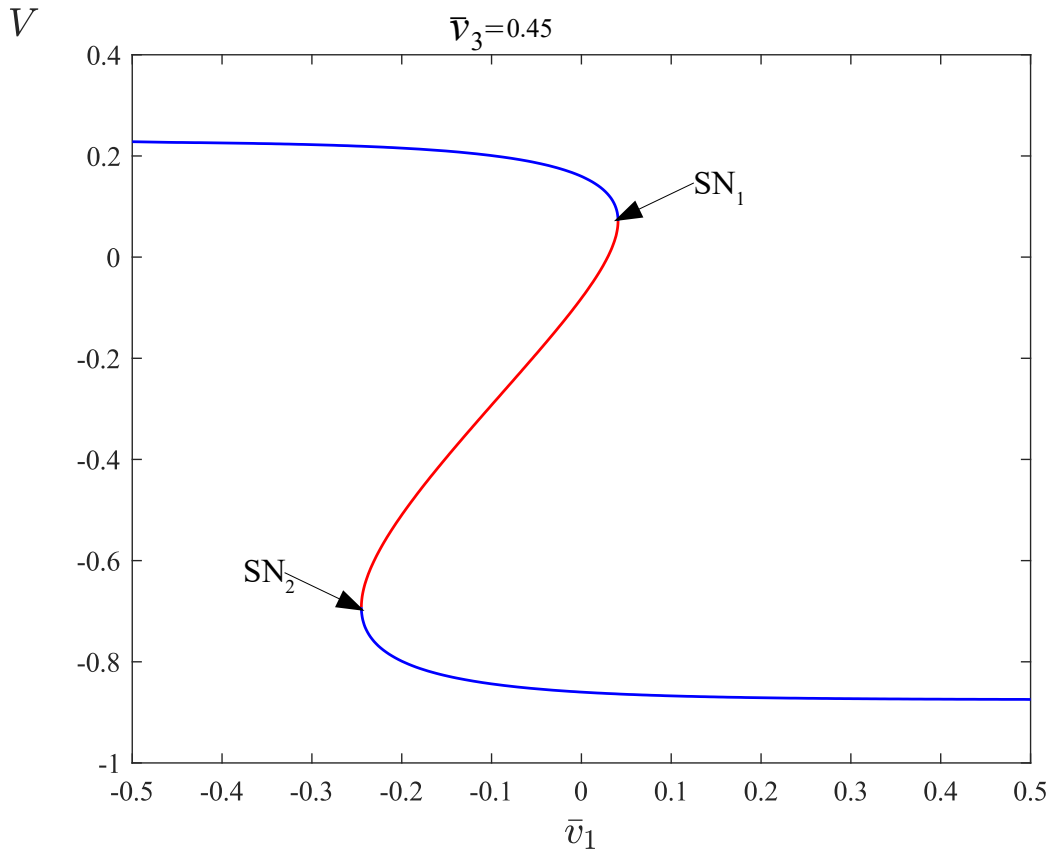

Figure: Transitions from Type I and II excitability

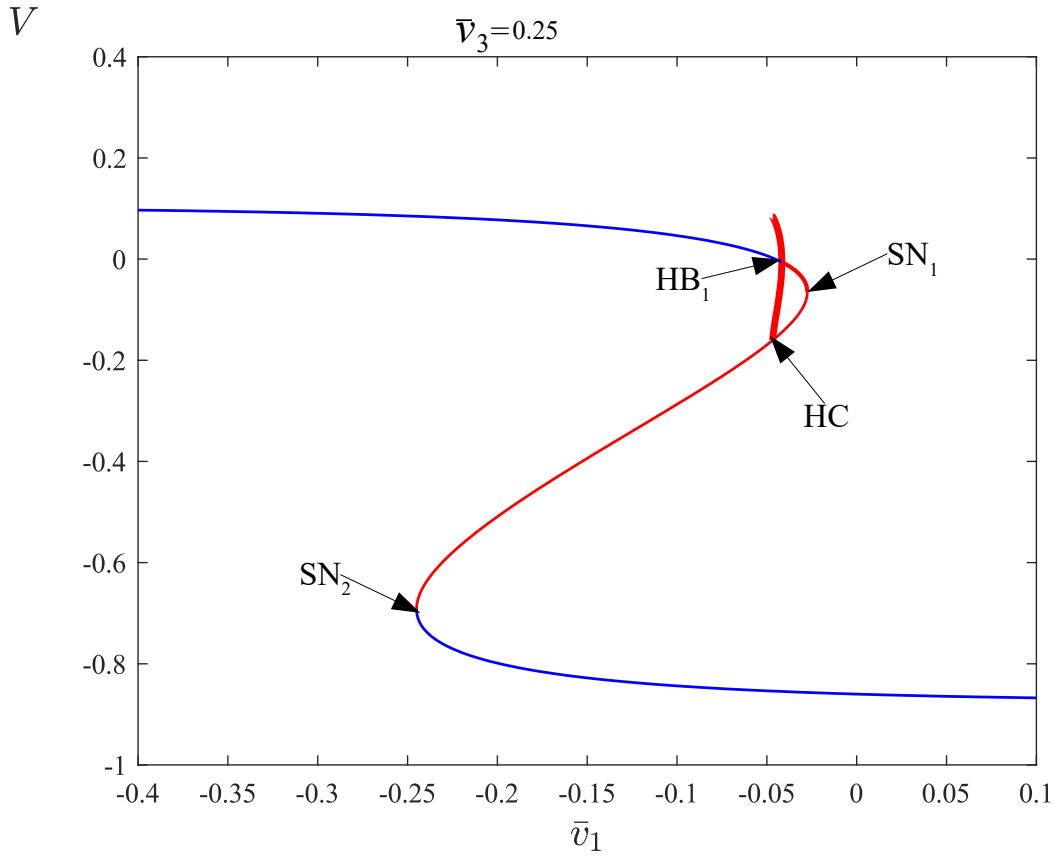

Figure: Transitions from Type I and II excitability

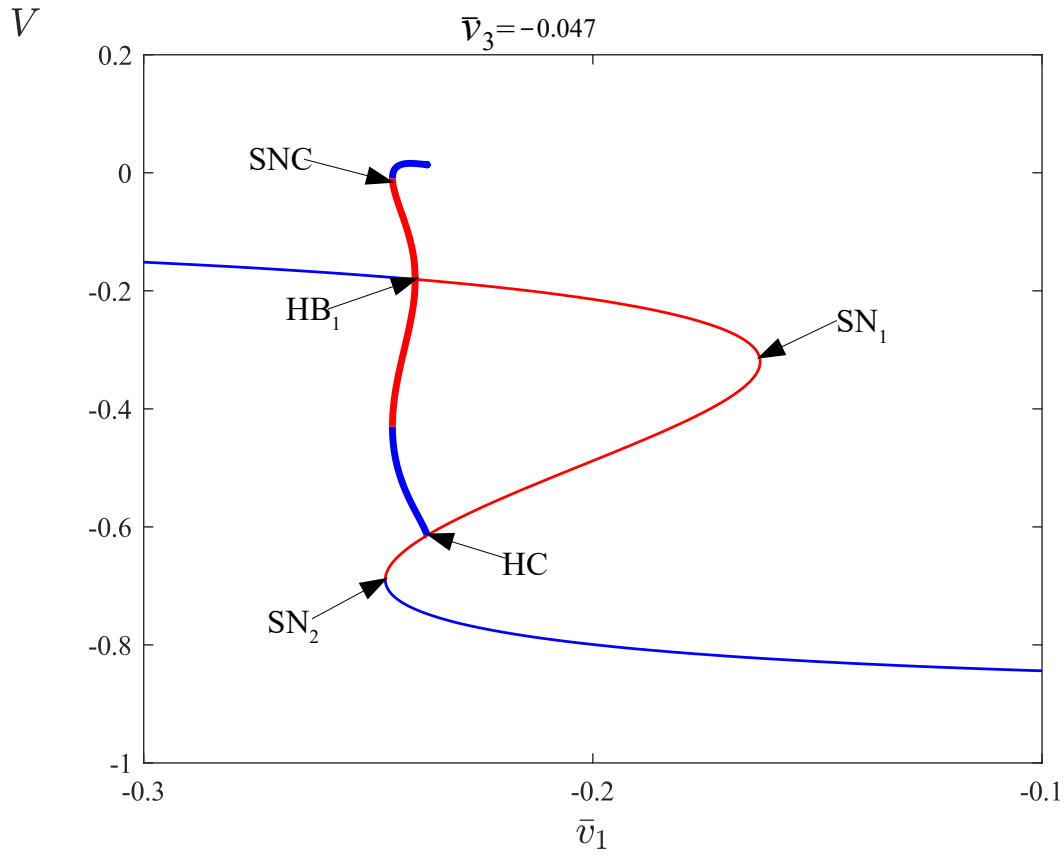

Figure: Transitions from Type I and II excitability

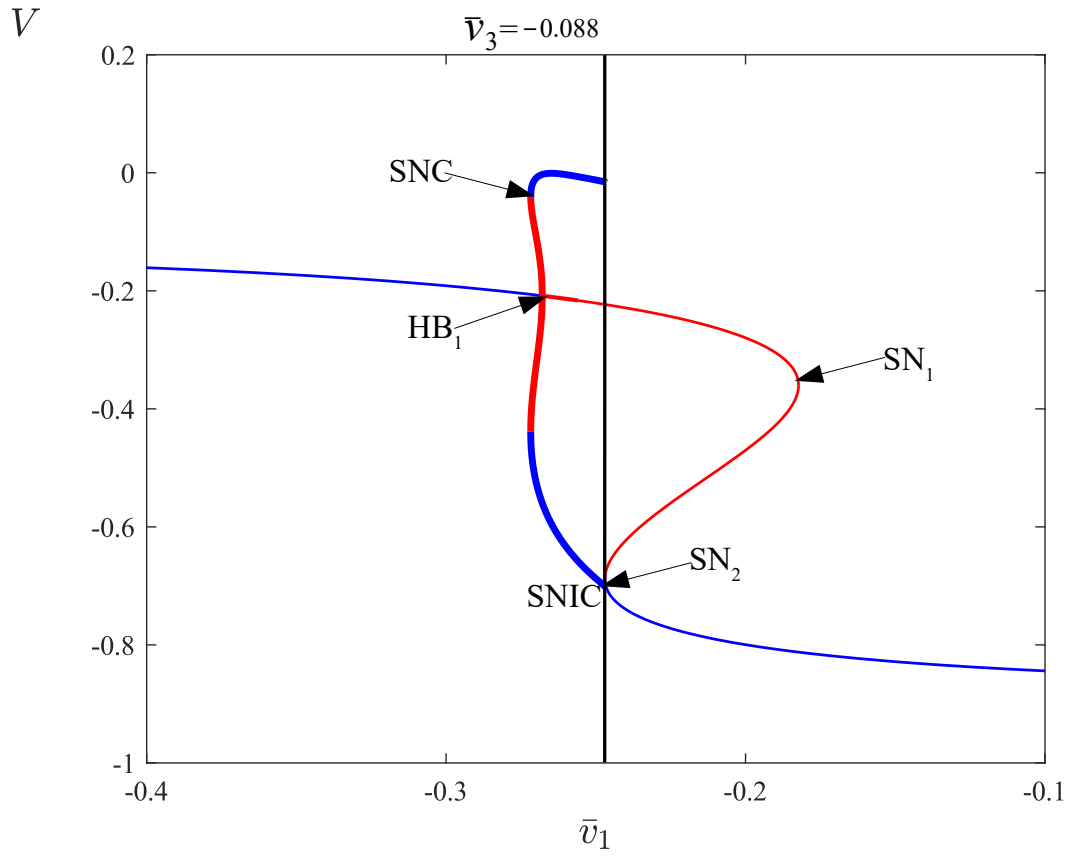

Figure: Transitions from Type I and II excitability

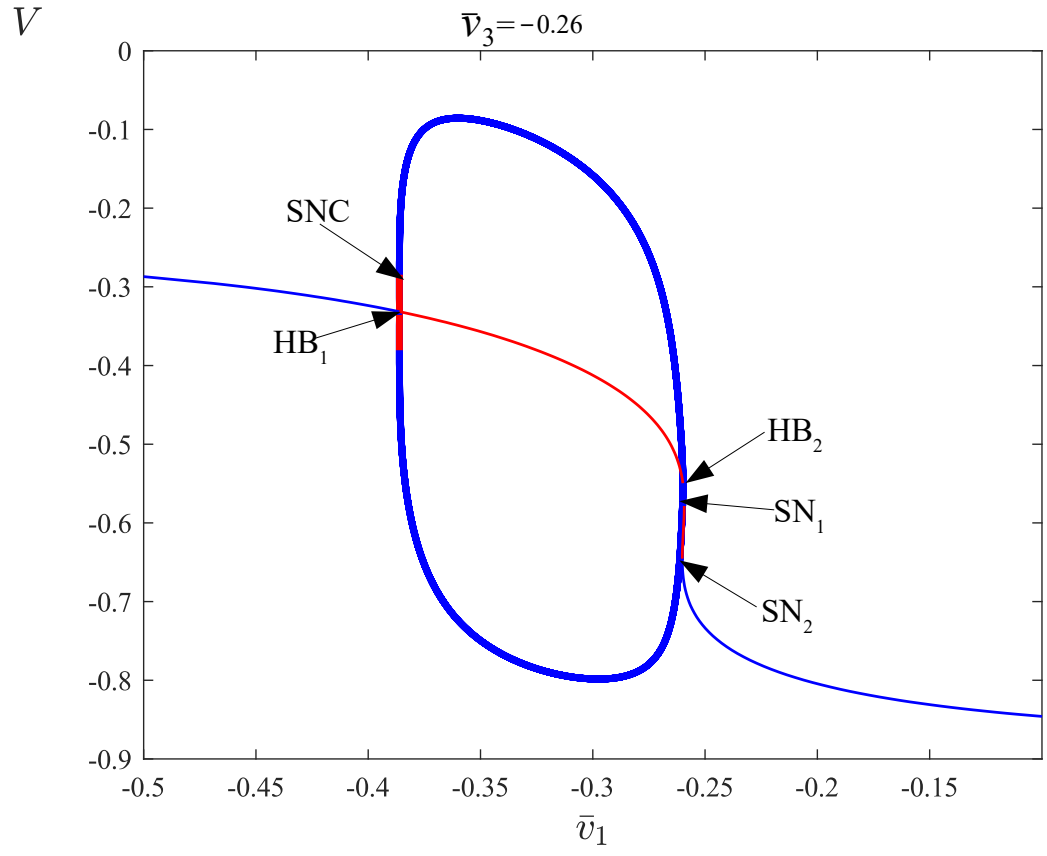

Figure: Transitions from Type I and II excitability

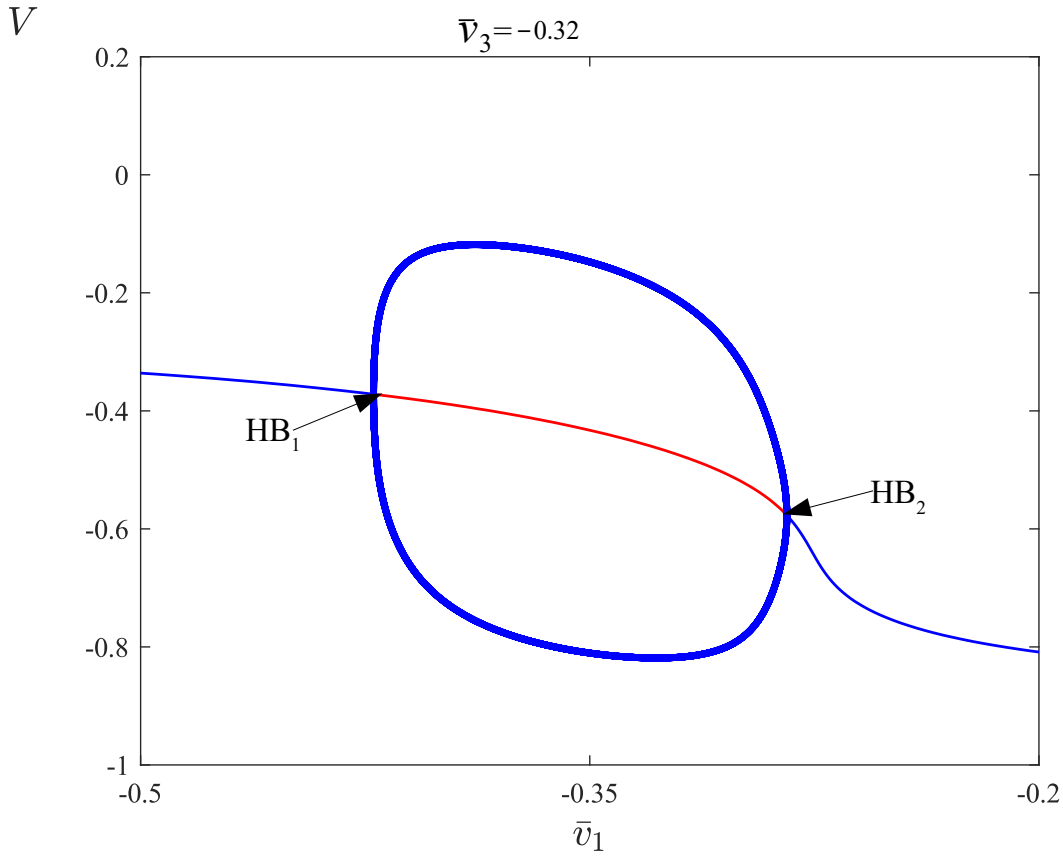

Figure: Transitions from Type I and II excitability

Coupled SMCs Model

$$\frac{\partial V}{\partial \tau} = D\frac{\partial^2 V}{\partial X^2} - \bar{g}_L(V - \bar{v}_L) - \bar{g}_K N(V - \bar{v}_K) - \bar{g}_{ca} M_\infty(V)(V - 1), \quad (6)$$

$$\frac{\partial N}{\partial \tau} = \lambda_N(V)\big(N_\infty(V) - N\big), \quad (7)$$

where V is the membrane potential, N is the fraction of open potassium channels, and

$$M_\infty(V) = 0.5\left(1 + \tanh\left(\frac{V - \bar{v}_1}{\bar{v}_2}\right)\right),$$

$$N_\infty(V) = 0.5\left(1 + \tanh\left(\frac{V - \bar{v}_3}{\bar{v}_4}\right)\right),$$

$$\lambda_N(V) = \psi \cosh\left(\frac{V - \bar{v}_3}{2\bar{v}_4}\right),$$

with no-flux boundary conditions and initial conditions:

$$V(0, X) = V_0(X) \text{ and } N(0, X) = N_0(X), \forall\ X \in \Omega.$$

Variation of model parameters results in wide range of spatiotemporal patterns including

- stationary inhomogeneous patterns
- travelling pulses
- fronts with spatiotempoaral chaos

Variation of $\bar{v}_1$

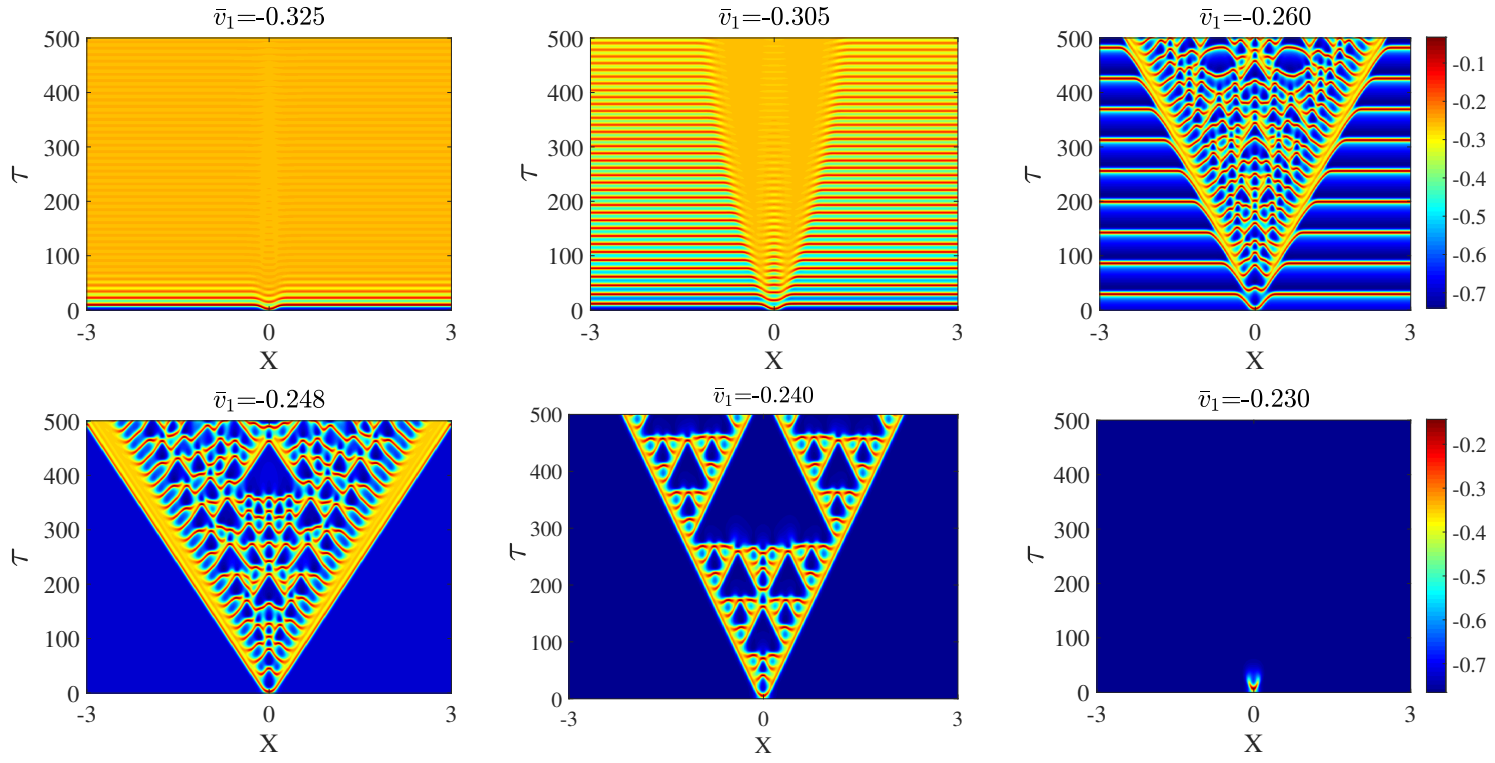

Figure 8: Space-time plot of the membrane potential V for selected values of parameter $\bar{v}_1$

Variation of ψ

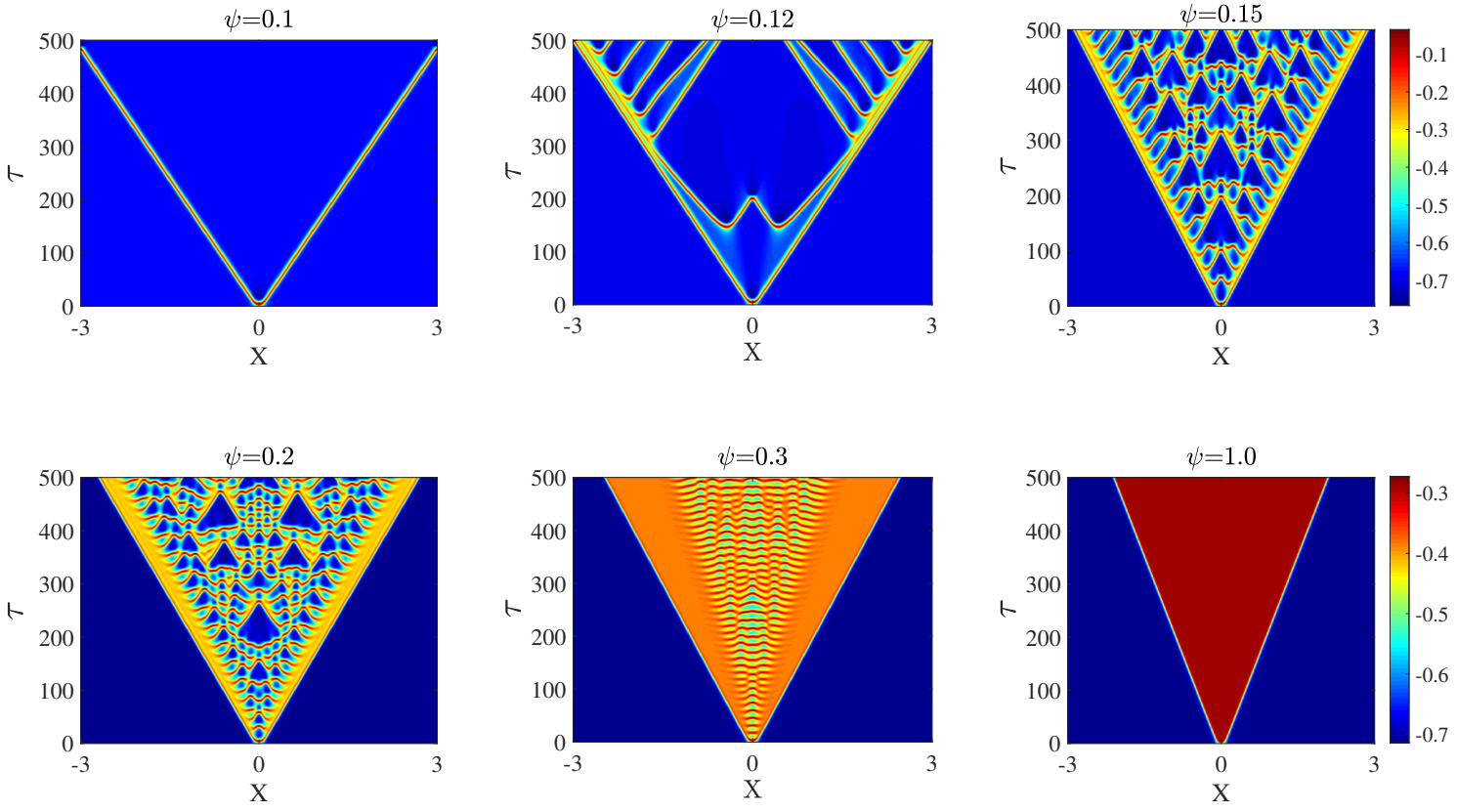

Figure 9: Space-time plot of the membrane potential V for selected values of parameter ψ

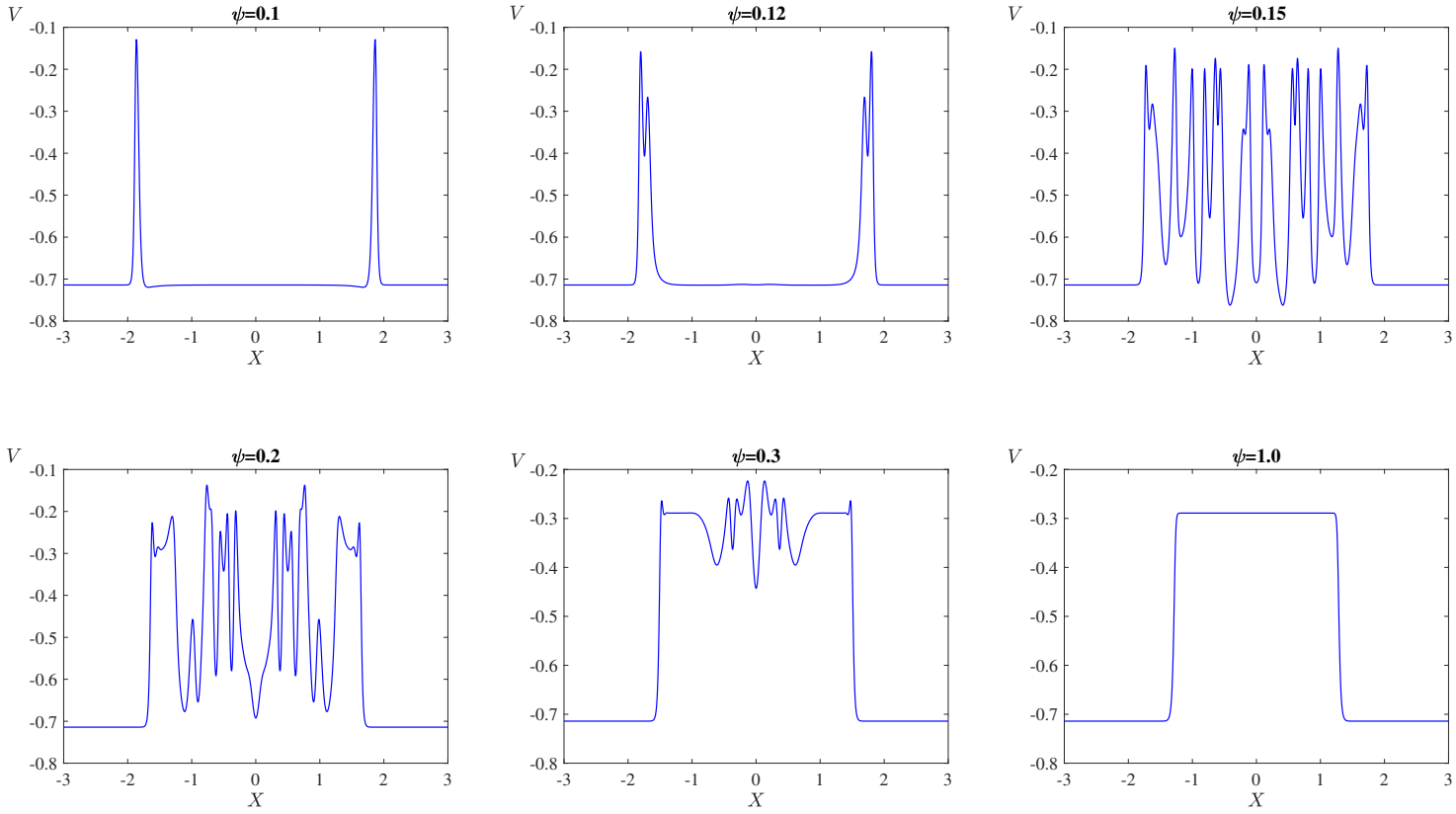

Figure 10: Solution profiles at time $\tau = 300$ showing the transitions from travelling pulses to spatiotemporal chaos and to fronts.

Summary

- We investigated the role of physiological parameters on EMC activity of SMCs in feline cerebral arteries.
- We found that the EMC is regulated by model parameters not external sources.
- Our results indicate that in some parameter regimes the coupled cells exhibit spatiotemporal chaos.
- These results could be useful in improving the understanding of physiological responses and disorders in smooth muscle cells.

Future work

- It remains to analyse the spectral stability of the travelling wave solutions observed in the model.

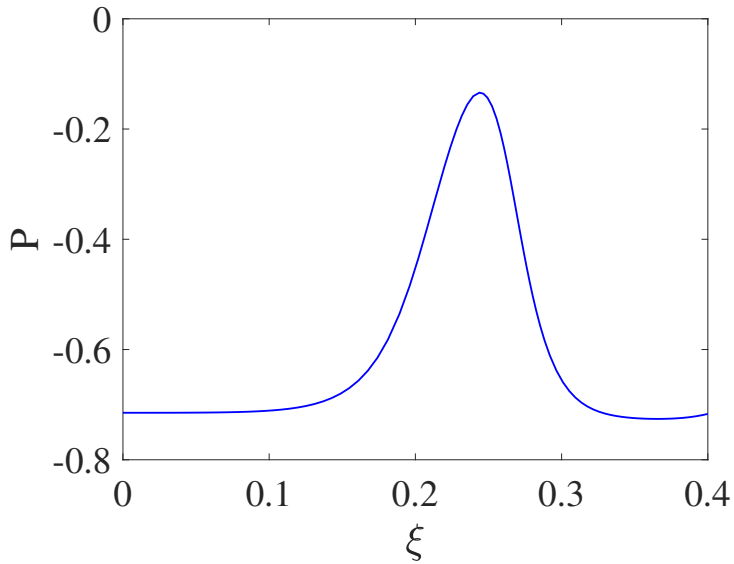

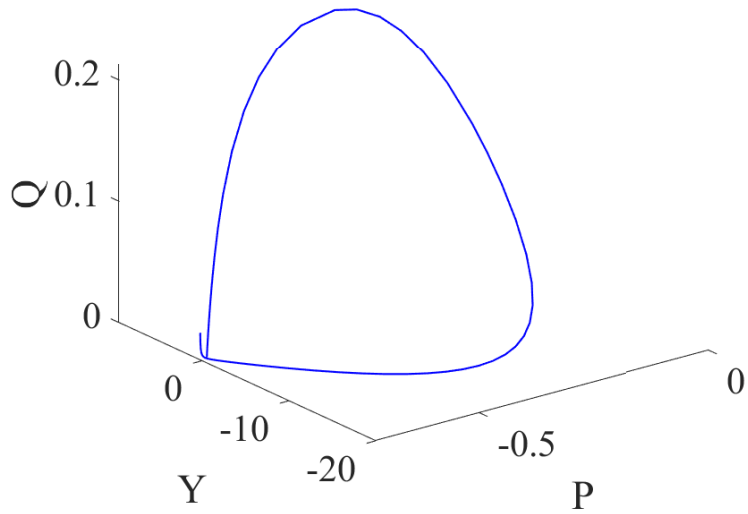

- Modify the model by incorporating the Na^+ inward current.

Acknowledgements

My Supervisors:

- Dr Richard G. Brown
- Dr David D.J.W. Simpson
- Ass. Prof. Bruce van Brunt

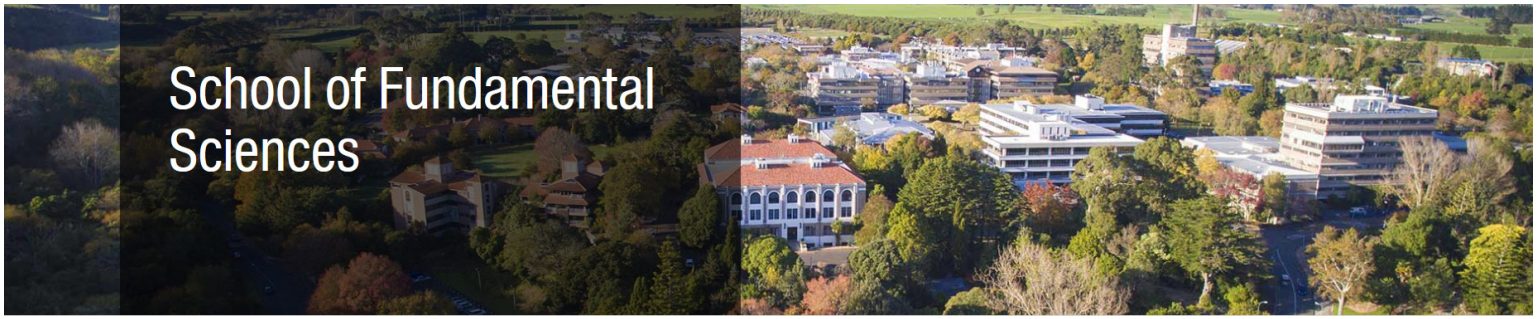

Thank you for your attention

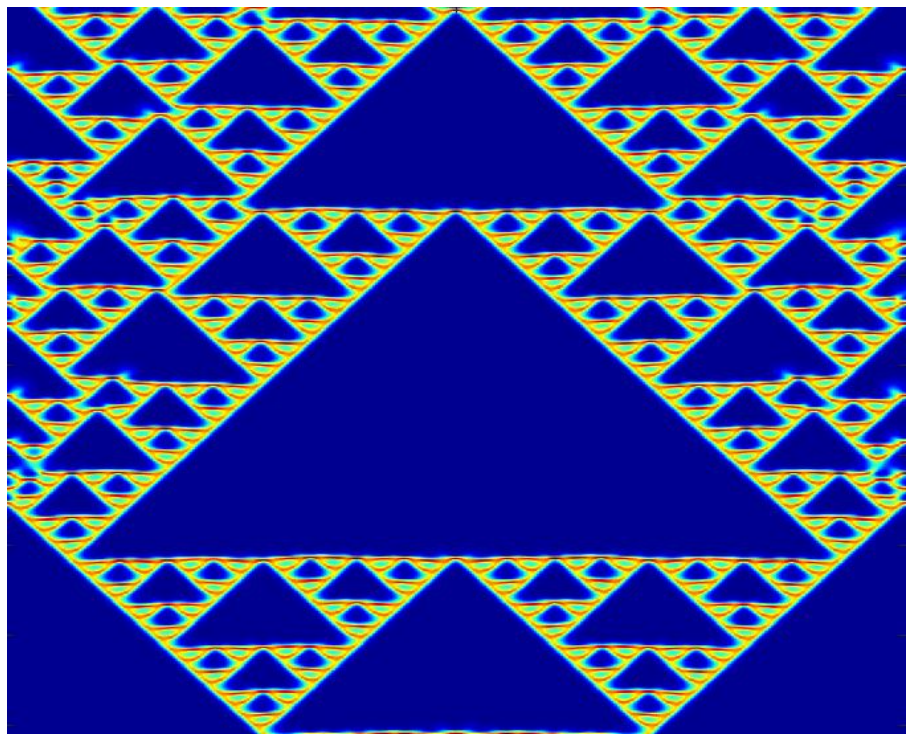

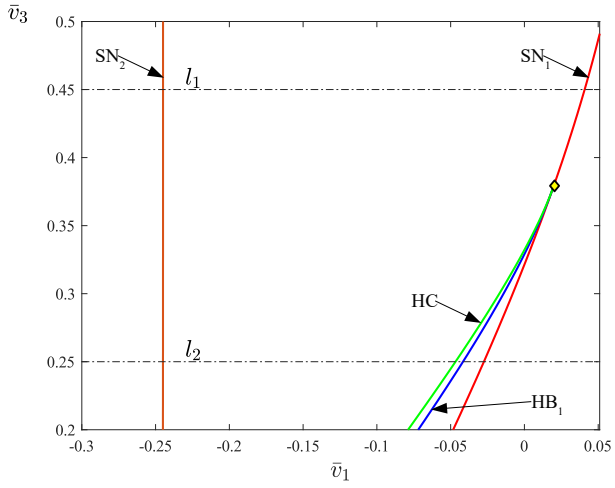
$\bar{v}_3$
SN$_2$
l_1
SN$_1$
HC
l_2
HB$_1$
$\bar{v}_1$

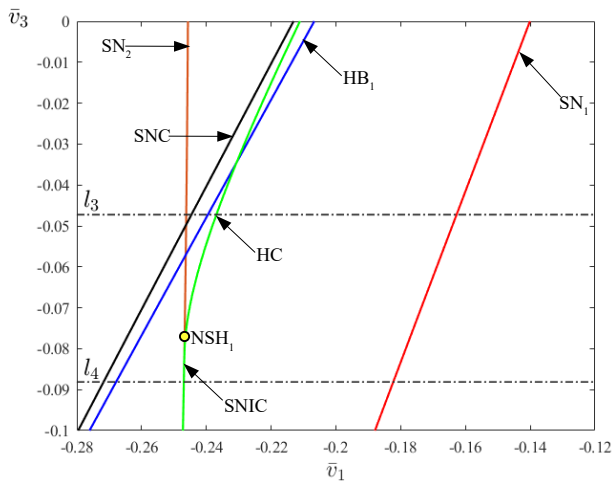
$\bar{v}_3$
SN$_2$
HB$_1$
SN$_1$
SNC
l_3
HC
NSH$_1$
l_4
SNIC
$\bar{v}_1$

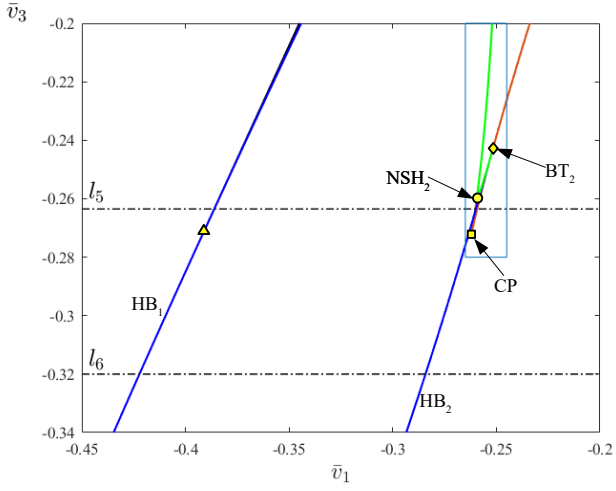
$\bar{v}_3$
NSH$_2$
BT$_2$
l_5
CP
HB$_1$
l_6
HB$_2$
$\bar{v}_1$

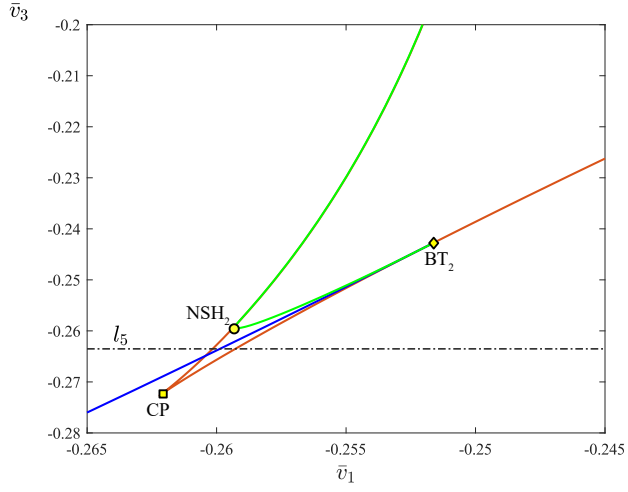
$\bar{v}_3$
BT$_2$
NSH$_2$
l_5
CP
$\bar{v}_1$

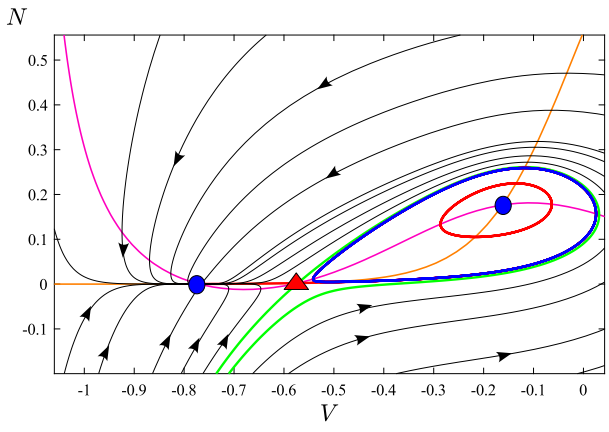
N
0.5
0.4
0.3
0.2
0.1
0
-0.1
-1
-0.9
-0.8
-0.7
-0.6
-0.5
-0.4
-0.3
-0.2
-0.1
0
V

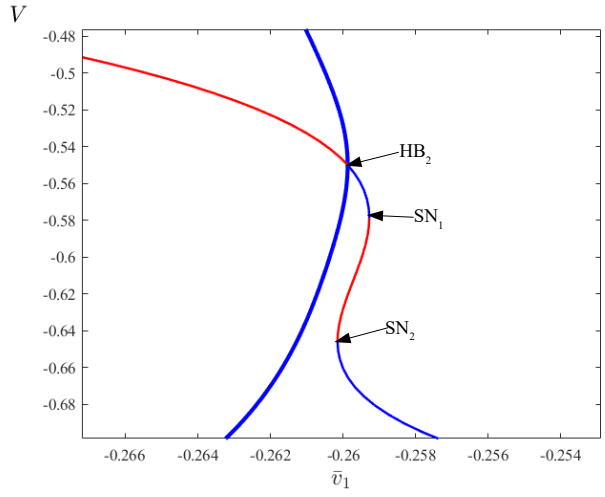
V
-0.48
-0.5
-0.52
-0.54
-0.56
-0.58
-0.6
-0.62
-0.64
-0.66
-0.68
HB2
SN1
SN2
-0.266
-0.264
-0.262
-0.26
-0.258
-0.256
-0.254
$\bar{v}_1$